Journal of Physiology (1993), **465**, *pp.* 121–147
With 13 figures
Printed in Great Britain

WHOLE-CELL K^+ CURRENTS IN FRESH AND CULTURED CELLS OF THE HUMAN AND MONKEY RETINAL PIGMENT EPITHELIUM

BY RONG WEN, GE MING LUI AND ROY H. STEINBERG

From the Departments of Physiology and Ophthalmology, University of California, San Francisco, CA 94143, USA

(*Received 27 May 1992*)

SUMMARY

1. Whole-cell potassium currents of freshly isolated human (adult and fetal) and monkey (adult) retinal pigment epithelial (RPE) cells, as well as cultured human and monkey RPE cells were studied using the patch-clamp technique.

2. In freshly isolated adult cells of both species, two currents were observed in the voltage range from −150 to +50 mV: an outwardly rectifying current and an inwardly rectifying current. These currents were also found in cultured cells of both species.

3. The outwardly rectifying current in freshly isolated adult human and monkey cells and some cultured cells was evoked by depolarizing voltage pulses more positive that −30 mV. The current activated with a sigmoidal time course after a brief delay, and was virtually non-inactivating. The conductance associated with the current was half-maximal at −16·4 mV for fresh human cells and −13·5 mV for fresh monkey cells, but was shifted 16·0 and 17·7 mV in the positive direction in cultured human and monkey cells, respectively. The reversal potential of the current in both human and monkey cells matched the potassium equilibrium potential (E_K) over a wide range of external potassium concentrations. This current was blocked by 20 mM tetraethylammonium.

4. A membrane current that exhibited inward rectification was observed with hyperpolarizing voltage pulses. The zero-current potential of this current was close to E_K. This current was blocked by 2 mM Ba^{2+} and 2 mM Cs^+. In cultured human and monkey cells, but not in fresh cells, this current exhibited an inactivation when voltage pulses were more negative than −120 mV. External Na^+ was responsible for the inactivation, as the inactivation was removed in a Na^+-free solution.

5. Membrane currents in freshly isolated fetal human RPE cells were remarkably different from those in adult cells. A transient outward current resembling the A-type potassium current was observed as the dominant membrane current in freshly isolated fetal human cells. This current activated when voltage pulses were more positive than −30 mV. It inactivated rapidly after reaching a maximal level. Application of 5 mM 4-aminopyridine (4-AP) completely blocked this current. Although this current was never observed in fresh adult cells, it was found in 33% of the cultured adult cells with similar kinetics, ion selectivity, and pharmacological properties.

MS 1399

6. In about 26% of the freshly isolated fetal human cells, a more slowly activating outward current, which resembled the delayed rectifier, was found to co-exist with the transient outward current.

7. The finding that the A-current was absent in freshly isolated adult human cells, while most of the fetal cells did not have the delayed rectifier or inward rectifier of adult cells, provides evidence, for the first time, that membrane-channel phenotype in RPE cells is developmentally regulated.

8. The occurrence of the A-current in cultured adult cells indicates that under culture conditions RPE cells undergo a change to the less differentiated, more neuroepithelial-like phenotype. Our findings support the hypothesis that de-differentiation occurs in human RPE cells in culture and may imply a potential capability of human RPE to regenerate neural retina as observed in other species.

INTRODUCTION

In the vertebrate retina the retinal pigment epithelium (RPE) supports the photoreceptors through an array of functions that includes metabolite, salt and water transport, and phagocytosis. RPE cells also are thought to have a glial-like relationship with rods and cones by responding to and changing the extracellular environment that surrounds them (for a review, see Steinberg, 1988). In particular, photoreceptor-induced changes in extracellular K^+ concentration alter RPE transport of salt and water, and these, in turn, modify the microenvironment. These functions are carried out, in part, by the ion channels and transport molecules of the apical (photoreceptor side) and basal (blood side) membranes of RPE cells, which have been characterized in microelectrode and isotope flux experiments (Miller & Steinberg, 1977*a*, *b*; Oakley, Miller & Steinberg, 1978; La Cour, Lund-Andersen & Zeuthen, 1986; Quinn & Miller, 1992; Lin, Kenyon & Miller, 1992). Recent patch-clamp recordings from isolated RPE cells have identified several voltage-sensitive currents. Whole-cell recordings from freshly isolated frog RPE cells (Hughes & Steinberg, 1990) revealed two voltage-dependent K^+ currents, an inwardly rectifying current and a delayed rectifier, and the latter also was clearly identified in freshly isolated turtle cells (Fox & Steinberg, 1992).

Human RPE cells are readily cultured, and what we know about the physiology of the human RPE has come primarily from studying cultured cells. Fox, Pfeffer & Fain (1988), in the one previous study of cultured human RPE with the patch-clamp technique, mainly performed single-channel recordings, and identified several types of voltage-independent K^+ currents. However, there have been no previous descriptions, to our knowledge, of potassium currents present in fresh human RPE cells by the patch-clamp technique.

The overall goal of the present work was to characterize the membrane potassium currents of freshly isolated human RPE cells, and to compare them to those of cultured cells. We were also able to perform a similar study on Rhesus monkey, fresh and cultured adult RPE cells, adding a comparison between primate species to our analysis. Our findings show a clear identity between the currents of fresh human and monkey adult cells, and an obvious similarity to those of cold-blooded vertebrates (Hughes & Steinberg, 1990; Fox & Steinberg, 1992). Interestingly, we found that membrane currents in fresh fetal human RPE cells differed remarkably from those

in fresh adult cells, indicating that membrane channel phenotype of RPE cells is developmentally regulated. We also observed distinct changes in cultured cells, the most remarkable of which was the occurrence of the A-current in cultured adult cells, which also was present in fresh fetal cells. Following the work of Neill & Barnstable (1990), we hypothesized that the presence of the A-current in culture represents a dedifferentiation of the cultured RPE cell towards the more primitive neuroepithelial channel phenotype present in the developing retina.

Some of this work has been presented previously in preliminary form (Wen, Lui & Steinberg, 1991*a*, *b*).

METHODS

Cell isolation and culture

Adult Rhesus monkey eye tissues were obtained from animals used for neuroscience experiments that had not involved the eye (provided by Drs H. J. Ralston III and D. B. Ralston). All animals were housed and cared for according to NIH and USDA regulations and protocols approved by the Committee on Animal Research, University of California, San Francisco (UCSF). Enucleation was performed under full anaesthesia immediately before the animals were killed. Induction was by ketamine (10 mg/kg, I.M.) followed by Nembutal (total 10–35 mg/kg, I.V.); the dose of Nembutal was increased until deep state III surgical anaesthesia was obtained, evidenced by absence of nociceptive reflexes and slow, deep respirations at a regular rate.

Adult human eye tissue (18–89 years of age, autopsy specimens) were obtained from the University of California Tissue Bank. Human fetal eye tissue (16–21 weeks of age) was obtained from second trimester aborted fetuses through the Reproductive Endocrinology Center, UCSF. All procedures were approved by the Committee on Human Research, UCSF.

RPE–choroid tissue was dissected from the neural retina and sclera. RPE cells were then isolated by incubating pieces of RPE–choroid in Hanks' solution containing collagenase (100 unit/ml, type IV, Sigma) for 1 h (fetal tissue for 30 min) at 37 °C. After incubation, RPE cell sheets were dissected free from choroid with fine-tipped forceps under a dissecting microscope. Cell sheets so obtained were used either for immediate recording or for cell culture. For immediate recording, cell sheets were washed in CMF (calcium- and magnesium-free) Hanks' solution and then incubated in CMF Hanks solution containing 10 unit/ml papain for 5–10 min and washed again. Single cells and small patches of cells were obtained by gentle trituration of the enzyme-treated tissue with a fire-polished Pasteur pipette.

For culture, cell sheets were washed in Hanks' solution three times, then incubated in CMF Hanks' solution for 10 min. Great care was taken to keep RPE cell sheets free from possible contamination by choroidal cells. Single cells or small patches of cells were obtained by gently triturating cell sheets with a fire-polished Pasteur pipette. Cells so obtained were then transferred to 35 mm ECM (extracellular matrix)-coated culture plates containing Dulbecco's modified Eagle's medium supplemented with 15% fetal calf serum, 1 ng/ml basic fibroblast growth factor (bFGF), and antibiotics (Song & Lui, 1990). Cells were kept at 37 °C with 10% CO_2–90% air and fed every other day. After reaching confluence (usually 7–10 days), cells were harvested for recording or seeded onto new ECM-coated plates for further propagation. In the present work, we used cells of passage 1–4.

Solutions

The composition of the normal bathing solution was (mM): 120 NaCl, 25 $NaHCO_3$, 5 KCl, 5 glucose, 2 $CaCl_2$, and 1 $MgCl_2$. Test solutions were made by modifying the normal solution. Cs^+-, Ba^{2+}-, or 4-aminopyridine (4-AP)-containing solutions were made by adding CsCl, $BaCl_2$, or 4-AP directly to the normal solution. Tetraethylammonium chloride (TEA)-containing solution was made by adding TEA to the normal solution at the expense of NaCl. Potassium concentration ($[K^+]$) change was reached by varying the potassium and sodium in the normal solution (mM): for 1 mM $[K^+]$, 1 KCl and 124 NaCl; for 25 mM $[K^+]$, 25 KCl and 100 NaCl; for 150 mM $[K^+]$, 125 KCl, 25 $KHCO_3$, 0 NaCl and 0 $NaHCO_3$. A Na^+-free solution was made by replacing all the $NaHCO_3$ with $KHCO_3$, and all NaCl and KCl with choline chloride in the normal solution so that this solution contained 25 mM K^+. All solutions were equilibrated with 95% O_2–5% CO_2 and adjusted, if necessary, to a pH of $7{\cdot}40 \pm 0{\cdot}05$.

The composition of the normal internal solution in the patch pipette was (mM): 30 KCl, 100 potassium gluconate, 15 $KHCO_3$, 5·5 EGTA-KOH, 0·5 $CaCl_2$, 1 $MgCl_2$, 1 ATP, and 1 GTP. This solution was equilibrated with 95% O_2–5% CO_2 and had a pH of 7·20±0·05. All chemicals were purchased from Sigma Chemical Co. (St Louis, MO, USA).

Whole-cell recording

Recordings were made in a chamber (400–500 μl in volume) that had a glass coverslip bottom coated with poly-L-lysine. The chamber was mounted on the stage of an inverted microscope (IMT-2, Olympus Optical Co., Tokyo, Japan). Isolated RPE cells were transferred to the chamber and allowed to settle for 10 min before starting perfusion. Solutions were delivered to one end of the chamber by gravity feed through thick-wall tubing (Tygon R-3603, Norton Co, Akron, OH, USA) to minimize the loss of CO_2, and removed at the opposite end by suction. Perfusion rate was 1–2 ml/min. All experiments were performed at room temperature (20–22 °C) within 5 h of cell isolation.

The whole-cell variant of the patch-clamp technique (Hamill, Marty, Neher, Sakmann & Sigworth, 1981) was employed to record membrane currents. Patch pipettes were pulled from borosilicate glass capillaries (1511–M, o.d. = 1·5 mm, i.d. = 0·84 mm, Glass Company of America, Millville, NJ, USA) with a two-stage vertical puller (Narishige, Tokyo, Japan). The opening of a pipette was estimated by bubble test in ethanol using a 10 ml syringe (Corey & Stevens, 1983). We used pipettes with bubble values of 6·3–6·5 ml, corresponding to a resistance of 1–3 MΩ when filled with internal solution. Pipettes were then coated with Sylgard (Dow Corning, Midland, MI, USA). The tip of a pipette was fire-polished immediately before use. Cells having a shiny basal membrane under phase contrast microscopy were selected for recording, as they usually gave stable seals. By slightly touching the basal membrane of a cell with the pipette tip and applying gentle suction, gigaohm seals ($\geqslant$ 20 GΩ) were usually achieved. The seal was allowed to stabilize for about 1 min. The membrane patch was then ruptured by a slightly stronger suction pulse to establish the whole-cell configuration.

Whole-cell currents were recorded with a patch-clamp amplifier (EPC-7, List Electronic, Darmstadt/Eberstadt, FRG) with the low-pass filter set to 3 kHz. Pipette and membrane capacitances were neutralized by built-in transient cancellation circuits for all recordings except for membrane capacitance measurement in which the membrane capacitance neutralization was disabled. A Ag–AgCl electrode, serving as the reference, was connected to the bath through a short bridge filled with internal solution set in 4% agar. Command potentials were generated by an IBM compatible microcomputer with software control (pCLAMP, Axon Instruments, Burlingame, CA, USA). Signals were digitized on-line and stored on disc on the computer for subsequent analysis. Statistical data are presented as means±S.D.

RESULTS

The apical portion of a typical adult RPE cell appeared darkly pigmented and usually exhibited short processes. The basal portion of the cell could be distinguished from the apical part by a narrowing of the cell body. This part of the cell usually had a smooth and shiny membrane with little observable pigment and so recordings were made at the basal membrane. Figure 1 shows a typical freshly isolated adult monkey RPE cell under phase contrast microscopy. Freshly isolated human fetal cells were smaller in size and had less processes on the apical portion, but the polarity of a cell was easy to distinguish under phase contrast microscopy.

When freshly isolated RPE cells were transferred to an extracellular matrix coated culture plate, they usually anchored to the bottom and began to spread within 5 h. Active proliferation was observed the second day and cells lost their pigmentation while proliferating, presumably by dilution. Cells usually reached confluence within 7–10 days and then maintained a monolayer. They eventually regained their pigment and began to form 'domes' by 4 weeks in culture. We harvested cells for recording after they reached confluence, usually 7–10 days after seeding. Dissociated

RPE cells usually had a rounded shape and did not exhibit obvious polarity. Cultured RPE cells ranged in size from 15 to 35 μm and we chose to study medium sized cells (about 20 μm) that had a shiny membrane since these usually sealed well and membrane capacitance could be neutralized.

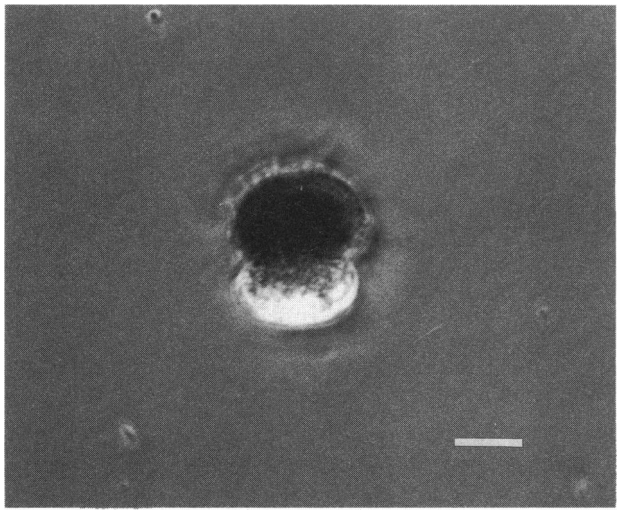

Fig. 1. Phase contrast photomicrograph of a freshly isolated adult monkey RPE cell. The apical portion of the cell is identified by the dense pigmentation and short processes. The basal part of the cell can be distinguished from the apical part by a narrowing of the cell body, and by its smooth membrane. Scale bar: 10 μm.

Membrane capacitance and resting potential

Cell membrane capacitance was estimated by a method modified from Jauch, Peterson & Läuger, (1986). In the absence of membrane capacitance neutralization, a voltage step of 10 mV produced a transient current that declined exponentially. The time constant of the current decline, τ, was assessed by fitting the declining phase with a single exponential curve. The membrane capacitance, C_m, was then calculated from the relation

$$C_m = \tau / R_{(in+s)}, \tag{1}$$

where $R_{(in+s)}$ is the equivalent resistance of the series resistance, R_s, and input resistance, R_{in}, in parallel:

$$R_{(in+s)} = R_s R_{in} / (R_s + R_{in}). \tag{2}$$

Calculated membrane capacitances are shown in Table 1. Cell resting potentials were measured under zero current-clamp condition immediately after breaking into the cell (junction potential was not subtracted). The reference potential was set by adjusting the tip potential to zero under zero current clamp with the pipette tip in the bath solution. Resting membrane potentials are also given in Table 1.

Membrane currents in freshly isolated and cultured adult human and monkey cells

We recorded from a total of forty-seven freshly isolated adult human cells and seventy-four freshly isolated adult monkey cells. Two distinct currents could be identified in all the fresh adult cells: a delayed outwardly rectifying current evoked by depolarization, and an inwardly rectifying current produced by hyperpolarization. Figure 2*A* shows a typical family of whole-cell currents from a fresh adult cell. The currents were recorded by holding a cell at −70 mV and clamping to voltages ranging from −110 to +50 mV in 20 mV increments.

TABLE 1. Cell membrane capacitance and resting potential

	Membrane capacitance (pF)	Resting potential (mV)
Fresh human adult cells	59·4 ± 10·0 (n = 21)	−50 ± 9 (n = 21)
Fresh human fetal cells	19·9 ± 9·0 (n = 42)	−34 ± 13 (n = 42)
Fresh monkey cells	63·3 ± 17·3 (n = 20)	−49 ± 10 (n = 20)
Cultured human cells	75·1 ± 17·3 (n = 25)	−40 ± 21 (n = 25)
Cultured monkey cells	79·3 ± 15·7 (n = 25)	−45 ± 15 (n = 25)

We recorded from more than 150 cultured human cells and over 80 cultured monkey cells. Three types of potassium currents could be identified in these cultured cells. Two of them closely resembled those found in freshly isolated cells. The third one, a fast transient outward current, was found in 33% of cultured human adult cells and in only one cultured monkey cell. Interestingly, this current was the dominant membrane current in *freshly* isolated *fetal* human cells (see below), but was never found in *freshly* isolated *adult* cells of both species.

Unlike in fresh cells, no clear pattern of membrane currents was observed in cultured cells. Some cells expressed only one type of current while others showed two or three types of currents. That some cells expressed only one type of current meant that we did not need to use special procedures to isolate such currents for study. Figure 2*B* shows a family of whole-cell currents from a cultured human cell that expressed two types of current: an outwardly rectifying current evoked by depolarization, and an inwardly rectifying current produced by hyperpolarization. Steady-state currents in Fig. 2*A* and *C* were measured as the average of data points between 850 and 950 ms and plotted in Fig. 2*B* and *D*, respectively, to show the current–voltage relationships.

Delayed rectifier

A delayed outwardly rectifying current was observed in all fresh cells while about 36% of cultured human and 41% of cultured monkey cells expressed this current. The current was evoked by depolarizing voltage pulses more positive than −30 mV. It activated slowly and was virtually non-inactivating. In many aspects, it resembled the delayed rectifier observed in excitable and other non-excitable cells.

Conductance

The conductance underlying the outward current, g, can be calculated from the following relation

$$g = I/(V_m - V_{rev}), \tag{3}$$

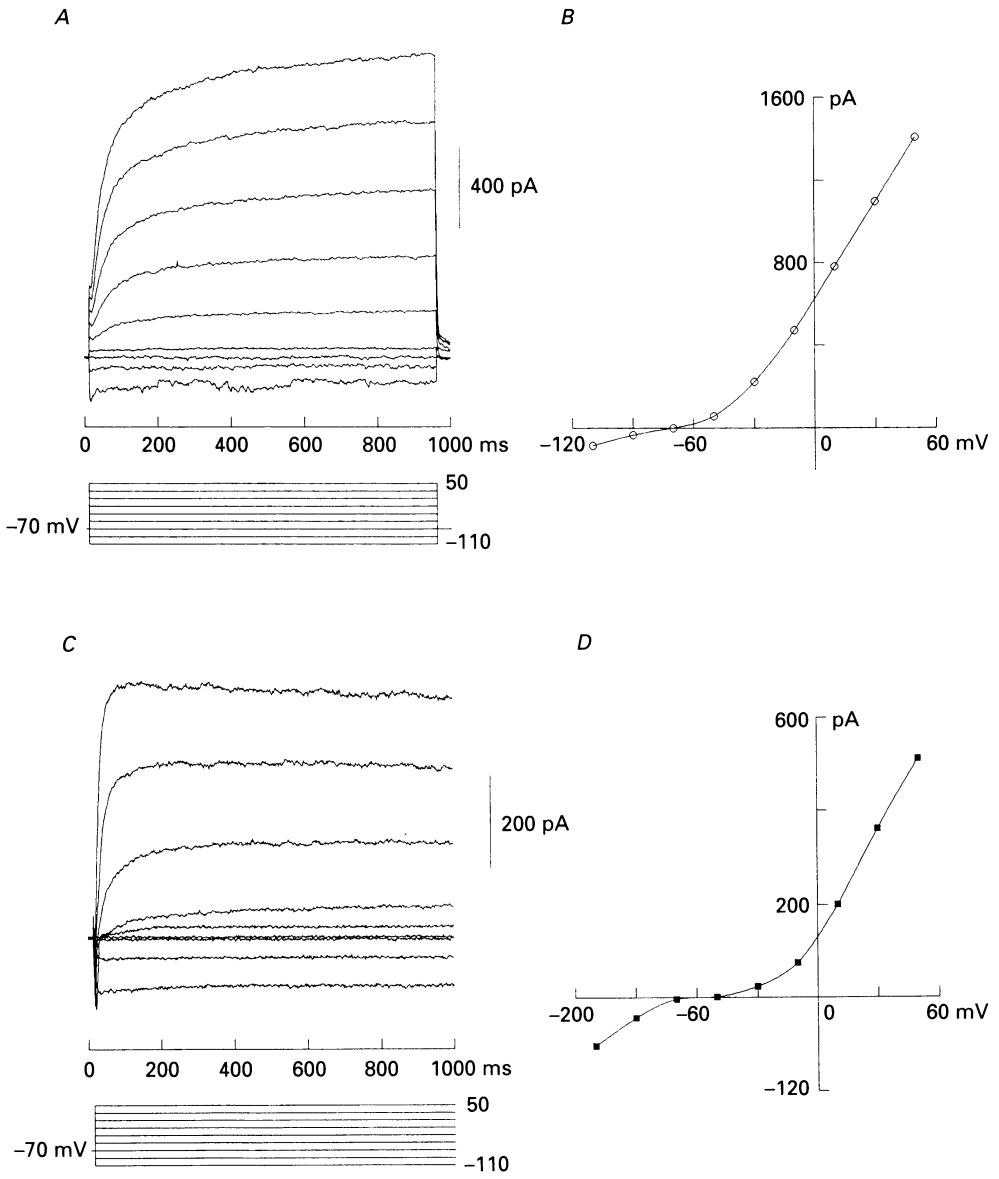

Fig. 2. Whole-cell currents in fresh and cultured adult RPE cells. *A* shows the whole-cell currents recorded from a fresh monkey RPE cell. Steady-state current in *A* was measured as the average of data points between 850 and 950 ms and plotted in *B* to show the *I–V* relationship. Whole-cell currents shown in *C* were recorded from a cultured human RPE cell and the *I–V* relationship is plotted in *D*. The current–voltage relationships in *B* and *D* exhibit both outward and inward rectification.

where I is the steady-state current at membrane potential V_m, and V_{rev} is the reversal potential of the current in normal external solution (−75 mV for fresh human cells and −80 mV for fresh monkey cells; −70 mV for cultured human cells and −80 mV for cultured monkey cells, see below). In Fig. 3*A*, the steady-state conductance at a

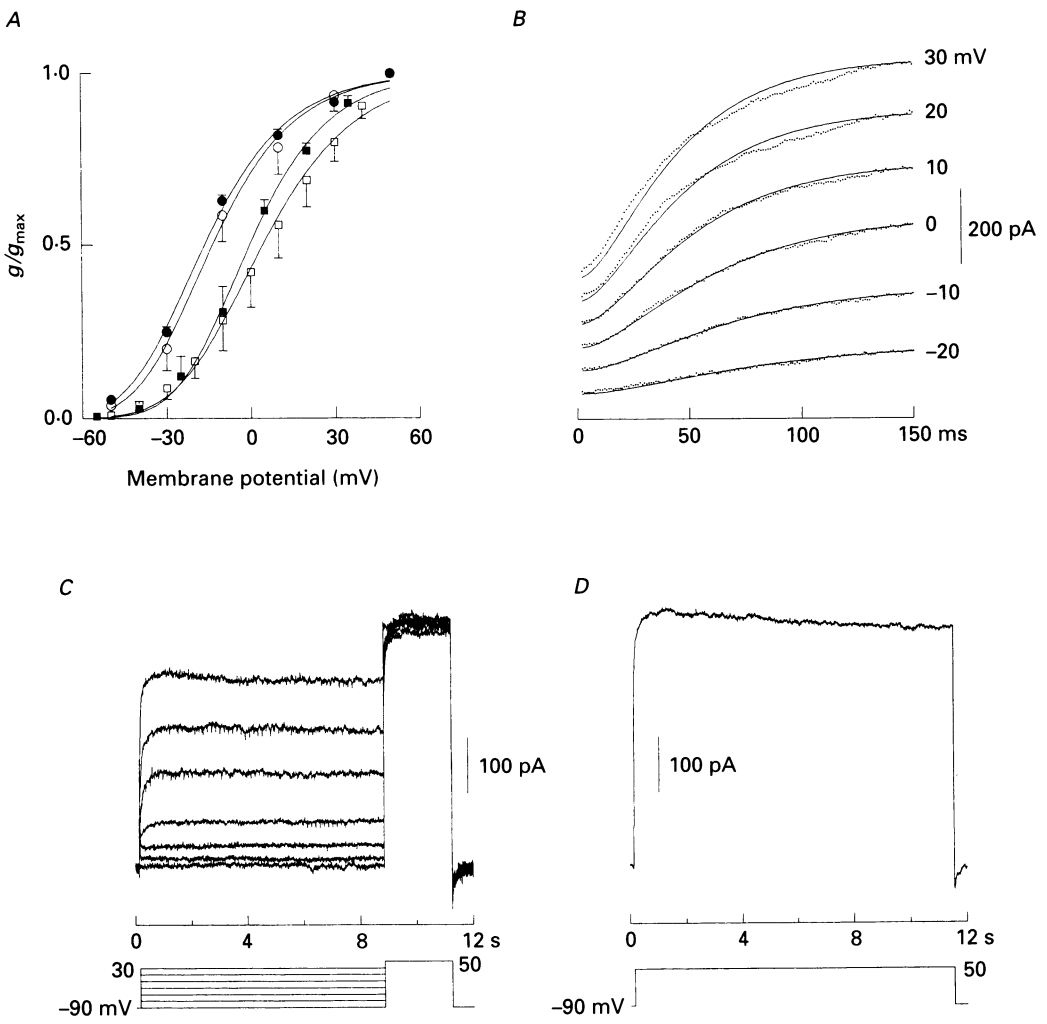

Fig. 3. Conductance–voltage relationships, activation, and inactivation of the delayed rectifier. In panel *A*, steady-state current at a given voltage was converted to conductance (g) using eqn (3), normalized to the conductance at +50 mV (g_{max}) and plotted to show the conductance–voltage relationship (●, fresh human cells, $n = 3$; ○, fresh monkey cells, $n = 11$; ■, cultured human cells, $n = 9$; and □, cultured monkey cells, $n = 11$). Data points were fitted to eqn (4) (continuous curves). Parameters used for curve fitting: fresh human cells, $V_{0.5} = -47{\cdot}4$ mV and $a = 18{\cdot}7$ mV/e-fold; fresh monkey cells, $V_{0.5} = -44{\cdot}0$ mV and $a = 18{\cdot}3$ mV/e-fold; cultured human cells, $V_{0.5} = -29{\cdot}8$ mV and $a = 17{\cdot}6$ mV/e-fold; cultured monkey cells, $V_{0.5} = -30{\cdot}4$ mV and $a = 20{\cdot}8$ mV/e-fold. Panel *B* shows the activation phase of the delayed rectifier from a fresh monkey cell. The outward current was evoked by voltage pulses of −20 to +30 mV (shown in the right column) from a holding potential of −70 mV. Data points were best fitted to eqn (5) (continuous curves). Panel *C* shows steady-state inactivation data. The amplitude of the current was virtually unaffected by the prepulse up to +30 mV. Panel *D* shows a current trace recorded by a +50 mV pulse of 11·5 s duration from the same cell as in *C*. At the end of this long voltage pulse, the current was reduced by only 7% from its maximal level. Results in panels *C* and *D* indicate that the current is non-inactivating.

given voltage (g) was calculated using eqn (3), normalized to the conductance at +50 mV (g_{max}), and plotted against membrane potential (●, fresh human cells; ○, fresh monkey cells; ■, cultured human cells; and □, cultured monkey cells). Data points were fitted to the equation

$$g/g_{max} = 1/\{1+\exp[(V_{0.5}-V_m)/a]\}^4, \quad (4)$$

where $V_{0.5}$ is the voltage at which a putative 'single-gate particle' (Hodgkin & Huxley, 1952) has a 50% probability at 'open' position, a is the slope factor (the voltage required to change the single-gate particle open probability e-fold). Channel conductance was half-maximal (mid-point of the fitting curve) at −16·4 mV for fresh human cells, −13·5 mV for fresh monkey cells, −0·4 mV for cultured human cells, and +4·2 mV for cultured monkey cells. The curves for the currents in fresh human and monkey cells closely parallel each other, indicating that the two currents had a strikingly similar voltage dependence. The same held for the currents in cultured human and monkey cells, where the curves also were a good match. Observe that the curves for currents in cultured cells were shifted to the right from those for currents in fresh cells, 16·0 mV for the current in cultured human cells and 17·7 mV for the current in cultured monkey cells, implying that RPE cells from the two species underwent similar change(s) in culture.

Activation and inactivation

When a depolarizing voltage pulse was applied, the current activated after a brief delay and followed a sigmoidal time course to reach its steady state. We analysed the activation of the current, in detail, in fresh cells. Figure 3*B* shows the activation phase of the current evoked by voltage pulses from −20 to +30 mV (holding potential (V_h) −70 mV). Each current trace (interrupted lines) was then fitted to the function (continuous lines).

$$I = I_{max}[1-\exp(-t/\tau)]^2, \quad (5)$$

where I_{max} is the amplitude of steady current, and τ is the time constant for activation. As the voltage pulses became more positive, the current activated more rapidly.

In fresh frog and turtle RPE cells, the outward potassium current showed strong inactivation (Hughes & Steinberg, 1990; Fox & Steinberg, 1992). However, the delayed outwardly rectifying currents in human and monkey cells, both fresh and cultured, exhibited only very small and slow, if any, inactivation. Steady-state inactivation of the current was studied, in detail, in fresh human and monkey cells. Figure 3*C* shows an experiment in which a series of prepulses ranging from −90 to +30 mV (in 20 mV increments) were applied to a cell prior to a test voltage pulse of +50 mV that evoked the outward current. As shown, even a prepulse of +30 mV failed to produce significant inactivation. Figure 3*D* shows a current trace recorded with an 11·5 s voltage pulse (+50 mV). At the end of this long voltage pulse, the current had only decreased to about 93% of its maximal amplitude. These findings indicated that the delayed outward rectifier in human and monkey RPE was virtually non-inactivating.

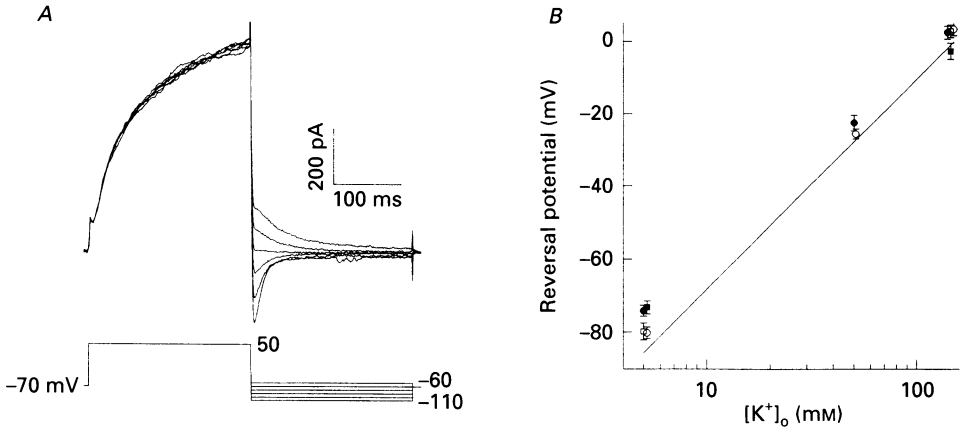

Fig. 4. Reversal potential of the delayed rectifier current and $[K^+]_o$. Tail current analysis was used to determine the reversal potential of the outward current in three K^+ concentrations: 5, 50, and 150 mM. Panel *A* shows a family of tail currents recorded from a monkey cell in 5 mM $[K^+]_o$. The main current was evoked by a depolarizing voltage pulse of +50 mV and was immediately stepped to potentials overlapping E_K. The tail currents so produced were measured and the interpolated zero intercept in the *I–V* plot (not shown) was taken as the reversal potential for each given $[K^+]_o$. Panel B is a semilogarithmic plot of reversal potentials of fresh human (●), fresh monkey (○), cultured human (■), and cultured monkey cells (□), against $[K^+]_o$. The continuous line represents E_K. Data points are from Table 2.

TABLE 2. Reversal potential of delayed rectifier

	5 mM $[K^+]_o$ (mV)	50 mM $[K^+]_o$ (mV)	150 mM $[K^+]_o$ (mV)
Fresh human adult cells	$-74{\cdot}1 \pm 2{\cdot}5$ ($n = 3$)	$-22{\cdot}5 \pm 2{\cdot}2$ ($n = 3$)	$2{\cdot}5 \pm 1{\cdot}8$ ($n = 3$)
Fresh monkey cells	$-80{\cdot}2 \pm 1{\cdot}6$ ($n = 3$)	$-25{\cdot}6 \pm 1{\cdot}4$ ($n = 3$)	$3{\cdot}4 \pm 1{\cdot}7$ ($n = 3$)
Cultured human cells	$-73{\cdot}2 \pm 1{\cdot}8$ ($n = 3$)	—	$-2{\cdot}6 \pm 2{\cdot}2$ ($n = 3$)
Cultured monkey cells	$-79{\cdot}8 \pm 2{\cdot}3$ ($n = 3$)	—	$2{\cdot}9 \pm 1{\cdot}7$ ($n = 3$)
E_K	−85·7	−27·7	0·0

Reversal potential and $[K^+]_o$

We performed tail current analysis to examine the reversal potentials of the delayed outwardly rectifying current in three external potassium concentrations ($[K^+]_o$): 5, 50 and 150 mM, in fresh human and monkey RPE cells, and in 5 and 150 mM $[K^+]_o$ in cultured human and monkey cells. The membrane potential of a cell was depolarized to +50 mV to activate the current (V_h −70 mV), and then stepped to test voltages that overlapped the potassium equilibrium potential (E_K) for a given $[K^+]_o$. Figure 4*A* shows a family of tail currents recorded in 5 mM $[K^+]_o$ from a fresh monkey RPE cell. The tail currents for a given $[K^+]_o$ were measured and then the interpolated zero intercept in the *I–V* plot (not shown) was taken as the reversal potential for that $[K^+]_o$ (Table 2). Figure 4*B* is a semilogarithmic plot of reversal potentials of the currents in fresh human (●) and monkey (○), and cultured human (■) and monkey cells (□). The reversal potential of the current for each cell type was close to E_K (Fig. 4*B*, continuous line). We concluded that the outward current was carried mostly by potassium.

Effects of external TEA

We further studied the outwardly rectifying current using a potassium channel blocker TEA. Our results showed that the current was significantly inhibited by extracellular application of 20 mM TEA. In the experiment shown in Fig. 5, families

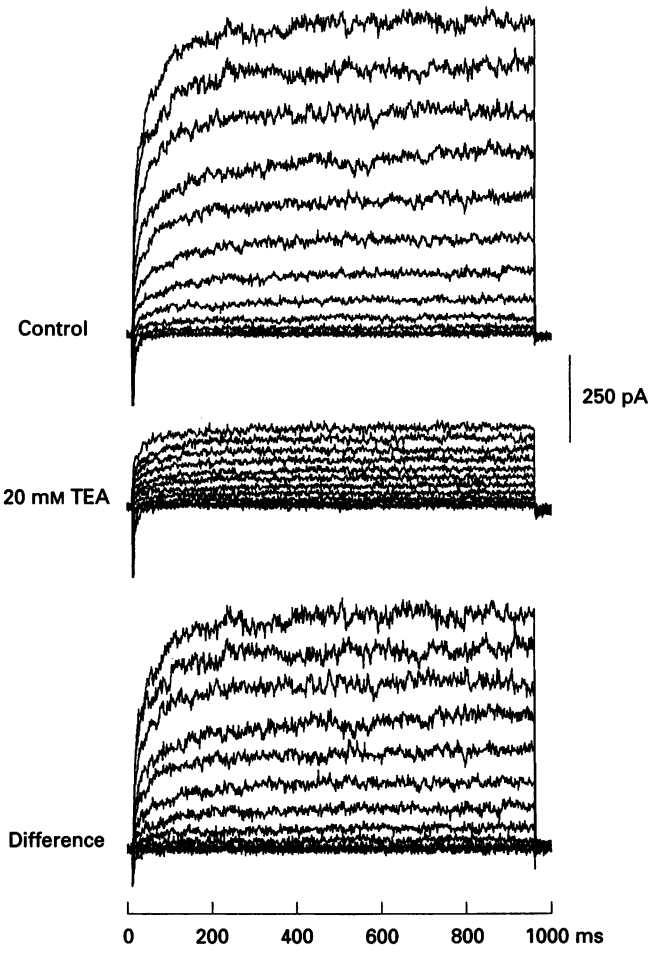

Fig. 5. Effect of TEA on the delayed rectifier current. A family of currents were recorded from a cultured monkey cell in control solution (upper panel). Another current family was recorded 4 min after application of 20 mM TEA (middle panel). A large portion of the current was blocked by TEA. Net TEA-sensitive current (lower panel) was obtained by subtracting the residual current after TEA from control current.

of the current were recorded from a cultured monkey cell with voltage pulses ranging from -50 to $+60$ mV in 10 mV increments (V_h -70 mV). The control recording was obtained when the cell was superfused with normal external solution (upper panel). The outwardly rectifying current was substantially reduced 5 min after 20 mM TEA application (middle panel). The lower panel of Fig. 5 shows net TEA-sensitive current, obtained by subtracting the current after TEA application from control current.

Inward rectifier

In all fresh adult human and monkey RPE cells, hyperpolarizing voltage pulses produced a current that showed an inwardly rectifying current–voltage relationship. This current activated very fast and then was maintained at the steady-state level for the entire duration of the voltage pulse. Figure 6*A* shows this current from a fresh human RPE cell. A family of currents was recorded by a series of voltage pulses ranging from −150 to −60 mV in 10 mV increments (V_h −50 mV). Steady-state current was measured as the average of data points between 200 and 250 ms in Fig. 6*A* and plotted in Fig. 6*B* to show the current–voltage relationship.

An inwardly rectifying current was also observed in 20% of cultured human and 14% of cultured monkey RPE cells. Although it was generally similar to the current in fresh cells, it differed by exhibiting a time- and voltage-dependent inactivation when voltage pulses were more negative than −120 mV. This inactivation was never observed in fresh cells. Figure 6*C* shows a family of currents from a cultured human cell, using the same voltage-clamp protocol as in Fig. 6*A*. Peak current (■) and steady-state current (▲, measured as the average of data points between 250 and 280 ms) in Fig. 6*C* were plotted in Fig. 6*D* to show both peak and steady-state current–voltage relationships. While the peak current was virtually a linear function of membrane potential, the steady-state current–voltage relationship showed a negative slope at membrane potentials more negative than −120 mV.

Zero-current potential and $[K^+]_o$

To confirm that the inwardly rectifying currents in both fresh and cultured cells were potassium currents, we assessed the zero-current potential in 1, 5 and 25 mM $[K^+]_o$, and the results showed that the zero-current potential of currents in fresh and cultured cells were both close to E_K (Table 3). We concluded that the inwardly rectifying currents in fresh and cultured cells are potassium currents.

Effects of Ba^{2+} *and* Cs^+

The inwardly rectifying currents of fresh and cultured cells were sensitive to the potassium channel blockers, barium and caesium. In Fig. 7*A*, a fresh monkey cell was first superfused with normal external solution while a family of currents was recorded by a series of voltage pulses ranging from −150 to −50 mV (upper panel). Another current family was recorded 5 min after application of 2 mM Ba^{2+} (middle panel). A substantial portion of the current was blocked by the application of Ba^{2+}, as shown by subtracting residual current after Ba^{2+} treatment from the control current (lower panel). Figure 7*B* illustrates effects of Cs^+ on the inwardly rectifying current for a cultured human cell, using the same protocol as in *A*.

Inactivation and Na^+

In tunicate egg cells and guinea-pig ventricular myocytes, inactivation of the inward rectifier was removed in Na^+-free solutions (Ohmori, 1978; Biermans, Vereecke & Garmeliet, 1988), indicating that Na^+ in the external solution was responsible for the inactivation. To determine if this was also the case for the inward current in cultured RPE cells, we studied inactivation of the current in a Na^+-free

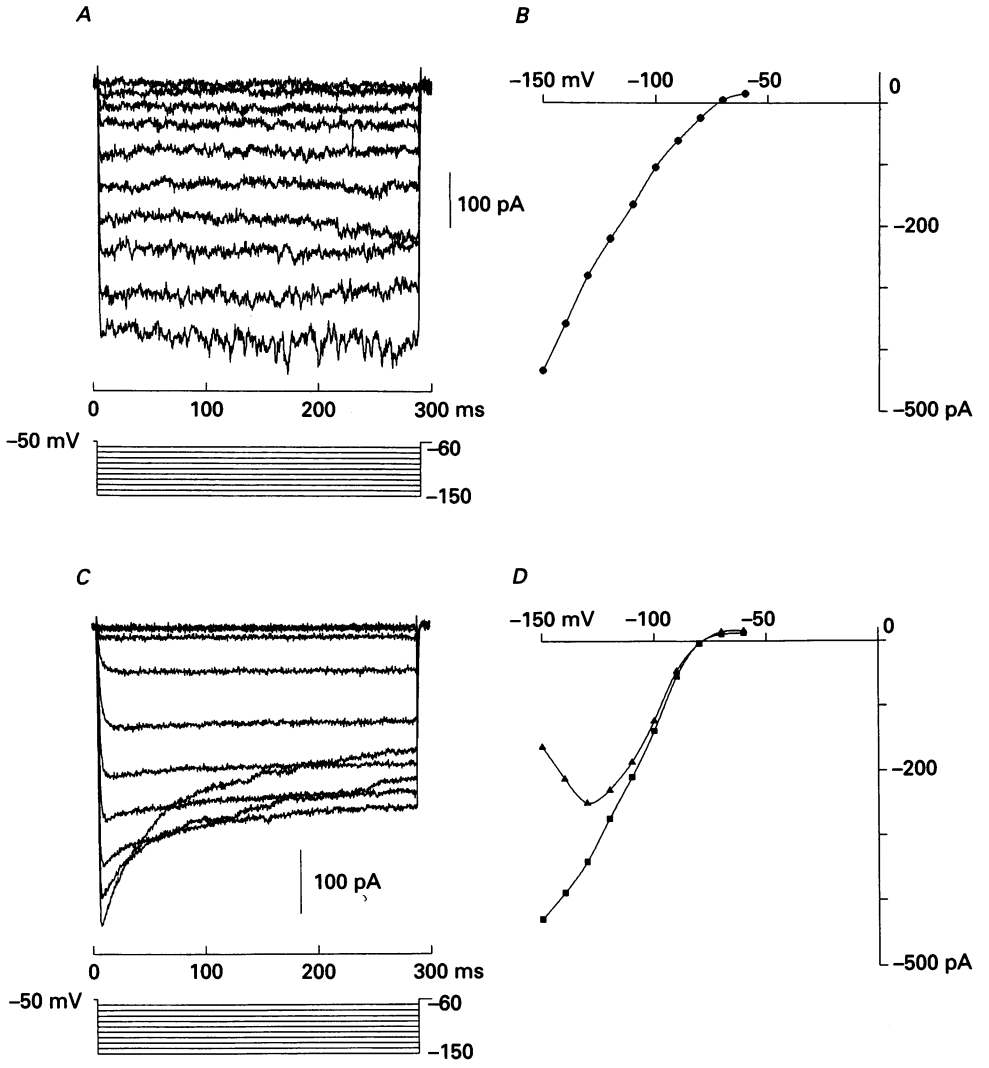

Fig. 6. Inward rectifier. Panel *A* shows a family of inwardly rectifying currents from a fresh human RPE cell. Steady-state current in *A* was plotted in *B* to show *I–V* relationship. Panel *C* shows the inwardly rectifying current from a cultured human cell. In panel *D*, peak (■) and steady-state current (▲) in *C* were plotted to show both peak and steady-state current–voltage relationships. Note that the inward rectifier in *C* exhibited a voltage- and time-dependent inactivation when the membrane potential was more negative than −120 mV.

TABLE 3. Zero-current potential of inward rectifier

	1 mM $[K^+]_o$ (mV)	5 mM $[K^+]_o$ (mV)	25 mM $[K^+]_o$ (mV)
Fresh adult human cells	−104·0±3·2 (n = 3)	−70·6±2·1 (n = 3)	−36·7±3·1 (n = 3)
Fresh monkey cells	−109·0±3·4 (n = 3)	−72·8±2·6 (n = 3)	−40·7±2·3 (n = 3)
Cultured human cells	−115·0±2·4 (n = 3)	−75·6±1·7 (n = 3)	−38·4±2·5 (n = 3)
Cultured monkey cells	−117·0±3·8 (n = 3)	−78·3±3·0 (n = 3)	−41·2±1·9 (n = 3)
E_K	−126·2	−85·7	−45·1 mV

solution containing 25 mM K^+, which was also the $[K^+]_o$ of the control solution. Figure 8*A* shows a family of currents recorded in the control solution from a cultured monkey RPE cell. The current was recorded by a series of voltage pulses ranging from −150 to −50 mV in 20 mV increments (V_h −50 mV). Substantial inacti-

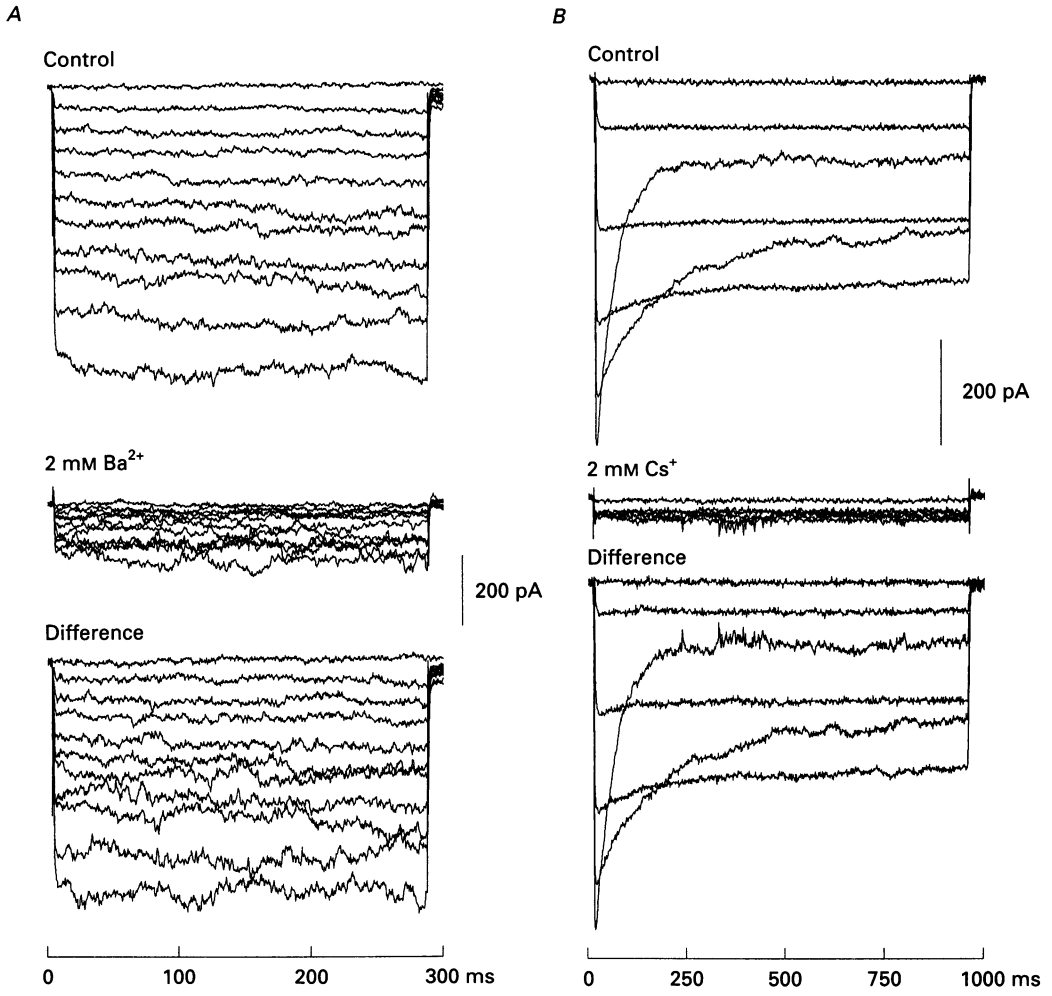

Fig. 7. Effects of Ba^{2+} and Cs^+ on the inward rectifier. Panel *A* shows the effect of Ba^{2+} on the inwardly rectifying current. A family of currents (upper panel) was recorded from a fresh human cell before application of 2 mM Ba^{2+}. Another current family was recorded 3 min after application of Ba^{2+} (middle panel). Net Ba^{2+}-sensitive current (lower panel) was obtained by subtracting the residual current after Ba^{2+} application from control. Panel *B* shows the effect of Cs^+. Data are from a cultured human cell. Current was recorded before (upper panel) and 5 min after application of 2 mM Cs^+ (middle panel). Net Cs^+-sensitive current (lower panel) was obtained by subtracting the residual current after Cs^+ application from control.

vation was observed in the current trace in response to the −150 mV voltage pulse. We then replaced the control solution with the Na^+-free solution and recorded another family of currents (Fig. 8*B*). The inactivation was almost completely

removed in the Na^+-free solution. Current traces in response to −150 mV voltage pulses were taken from Fig. 8*A* and *B* and superimposed in *C* (labelled as 'Control' and 'Na^+ free', respectively). These results clearly indicated that in cultured human and monkey RPE cells, the inactivation of the inward rectifier at very negative potentials was caused by external Na^+.

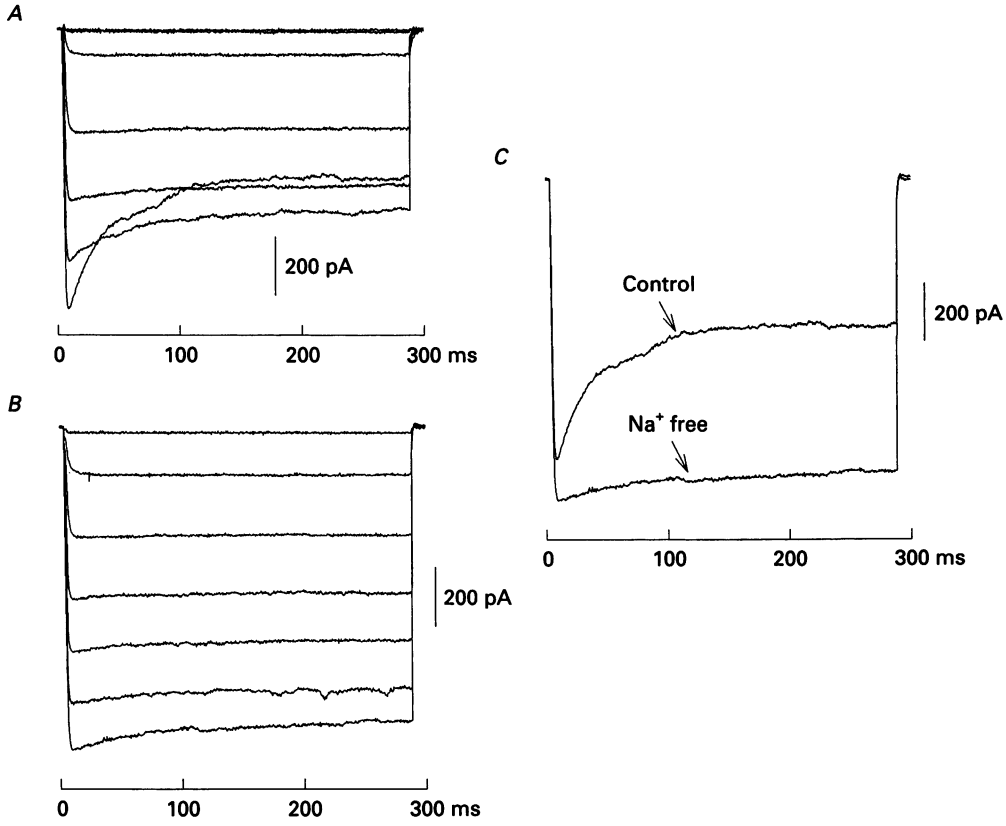

Fig. 8. Inactivation of the inward rectifier. Panel *A* shows a family of inward rectifier currents recorded from a cultured monkey cell in control solution. Substantial inactivation was seen in the current trace with 150 mV voltage pulse. In panel *B*, another family of currents was recorded 5 min after changing to a Na^+-free solution, using the same voltage-clamp protocol as in *A*. Inactivation was almost completely removed in the Na^+-free solution. Current traces with −150 mV voltage pulses in *A* and *B* are superimposed in panel *C*. The Na^+-free solution used in these experiments was made by replacing the 25 mM $NaHCO_3$ in the normal external solution with 25 mM $KHCO_3$, while the 120 mM NaCl and 5 mM KCl were substituted with 125 mM choline chloride so that it had 25 mM K^+. The control solution also contained 25 mM K^+.

Currents observed in fresh fetal human cells

We studied fifty-four freshly isolated fetal (16 to 21 weeks) human RPE cells (cell capacitances and membrane potentials are given in Table 1). The membrane currents in these cells differed remarkably from those in fresh adult cells. A fast transient outward current, which resembled the A-current (Rogawski, 1985; Rudy, 1988), was the dominant membrane current in these cells, while most of the cells did not exhibit

the delayed rectifier or inward rectifier. A similar fast transient current was found in 33% of cultured human adult cells, although it was absent in all fresh adult cells. In this section, we describe membrane currents in freshly isolated human fetal cells, and compare the fast transient current with the similar current in cultured adult human cells.

Fast transient outward current

In all the fresh human fetal cells studied, a fast transient outward current was observed when the cell membrane was depolarized to more positive than −30 mV from a holding potential of −100 mV. In most cells, this current was not significantly contaminated by other currents so that we did not need to use a special procedure to isolate it. Figure 9*A* shows a family of this current in an isolated cell. The cell membrane was held at −100 mV and then clamped to potentials ranging from −50 to +80 mV in 10 mV increments. Peak current in Fig. 9*A* was plotted against membrane potential to show the current–voltage relationship (Fig. 9*B*).

While most *cultured fetal* cells also expressed this current, we were surprised to find that 33% of *cultured* cells of *adult* origin exhibited this current, which was absent in all the *fresh adult* cells. Figure 9*C* shows a family of currents recorded from a cultured human cell derived from a 53 year old donor, using the same voltage-clamp protocol as in Fig. 9*A*. Peak current in Fig. 9*C* is plotted against membrane potential in Fig. 9*D* to show the current–voltage relationship.

Conductance and inactivation

The conductance underlying the transient outward potassium current, g, can be calculated from the following relation:

$$g = I_{pk}(V_m - V_{rev}), \tag{6}$$

where I_{pk} is the peak current at a given membrane potential V_m, and V_{rev} is the reversal potential of the current in normal external solution (−70 mV in 5 mM $[K^+]_o$, see below). In Fig. 10*A*, peak current at a given voltage was converted to conductance (g) using eqn (6), normalized to peak current at +50 mV (g_{max}), and plotted against membrane potential (●, fresh human fetal cells; ■, cultured human adult cells). The curves through data points in Fig. 10*A* (continuous curve, fresh human fetal cells; interrupted curve, cultured human adult cells) were the best fit to eqn (4) ($V_{0.5} = -42.8$ mV, $a = 20.2$ mV/e-fold for fresh human fetal cells; $V_{0.5} = -39.7$ mV, $a = 19.6$ mV/e-fold for cultured human adult cells). Channel conductance is half-maximal at −9·2 mV for fresh human fetal cells and −7·2 mV for cultured human adult cells (mid-points of the curves).

The transient outward current declined sharply after reaching its peak. The inactivation phase could be fitted with a single exponential curve and from the fitting curves, the time constant of inactivation at a given membrane potential could be determined. We found that there was no significant change in the time constant at membrane potentials from +20 to +80 mV, indicating that the time constant of inactivation was voltage independent.

The voltage dependence of steady-state inactivation was studied by applying a series of prepulses ranging from −90 to −35 mV (−90 to −10 mV for cultured human adult cells) and recording the peak current elicited by subsequent +50 mV

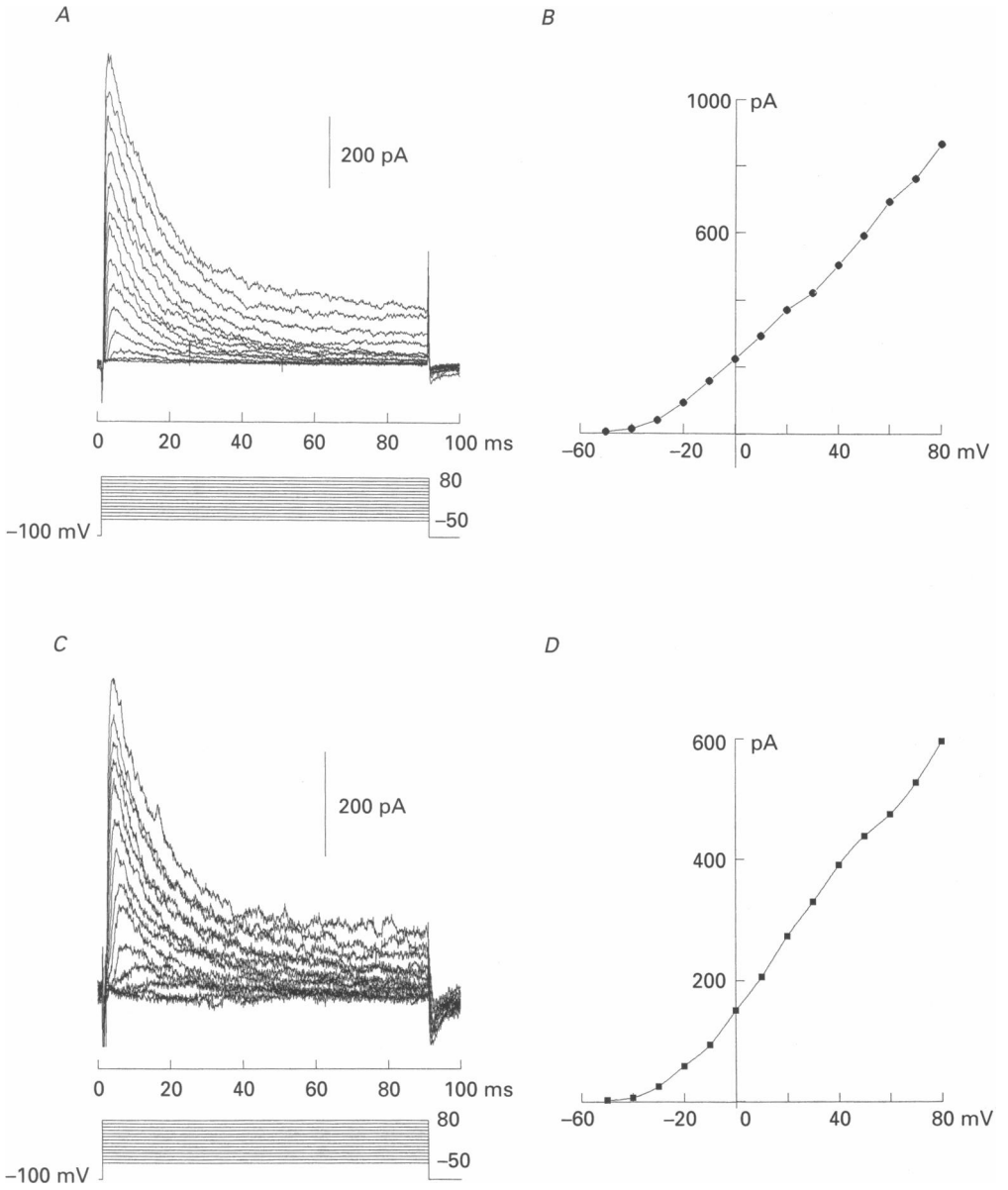

Fig. 9. Transient outward current. Panel *A* shows the transient outward current from a freshly isolated human fetal cell. Peak current taken from *A* was plotted in panel *B* to show the peak *I–V* relationship. Panel *C* shows the transient outward current from a cultured human cell derived from a 53 year old donor. Peak current in *C* was measured and plotted in panel *D* against the membrane potential to show the *I–V* relationship.

test pulses. In Fig. 10*B*, peak current for a given prepulse (I) was normalized to the peak current for a prepulse of -90 mV (I_{max}) and then plotted against prepulse voltage. The data points were fitted to a Boltzmann function:

$$I/I_{max} = 1/\{1+\exp[V_{prep}-V_{0.5})/a]\}, \quad (7)$$

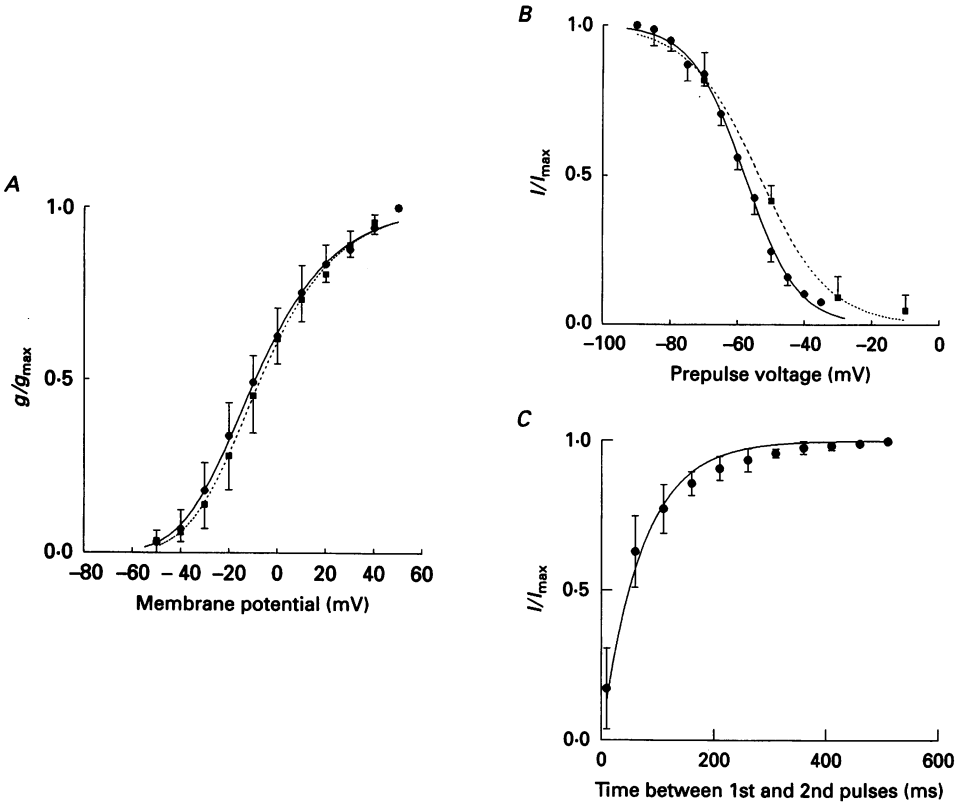

Fig. 10. Conductance–voltage relationship and inactivation of the transient outward current. In panel *A*, conductance at a given membrane potential (g) was calculated according to eqn (6) ($V_r = -70$ mV), normalized to the conductance at +50 mV (g_{max}), and plotted against membrane potential (●, fresh human fetal cells, $n = 4$; ■, cultured human adult cells, $n = 5$). The curves through data points are the best fit to eqn (4) (continuous curve, fresh human cells; interrupted curve, cultured human adult cells). Parameters used for curve fitting: $V_{0.5} = -42.8$ mV and $a = 20.2$ mV/e-fold for fresh human fetal cells; and $V_{0.5} = -39.7$ mV and $a = 19.6$ mV/e-fold for cultured human adult cells. The half-maximal conductance was at −9·2 mV for fresh human fetal cells and −7·2 mV for cultured adult human cells. Panel *B*, steady-state inactivation. Peak current (I) was normalized to the one at a prepulse of −90 mV (I_{max}), and plotted as a function of the prepulse voltage (●, fresh human fetal cells, $n = 4$; ■, cultured human adult cells, $n = 4$). The curves through data points are the best fit to a single Boltzmann function (eqn 7) (continuous curve, fresh human fetal cells; interrupted curve, cultured human adult cells). Parameters used for curve fitting: $V_{0.5} = -57.9$ mV and $a = 7.9$ mV/e-fold for fresh human fetal cells; and $V_{0.5} = -53.6$ mV and $a = 10.5$ mV/e-fold for cultured human adult cells. Panel *C*, recovery from inactivation at −100 mV. Data are from fresh fetal cells. The current was produced by a series of +50 mV double pulses of varying interval from −100 mV holding potential. Peak current produced by the second pulse (I) was normalized to the one evoked by the first pulse (I_{max}) and plotted as a function of the time interval between the two pulses ($n = 5$). The continuous curve through the data points is the best fit to eqn (8). The time constant of recovery from inactivation at −100 mV was 71·0 ms.

where V_{prep} is the prepulse voltage, $V_{0.5}$ is the prepulse voltage at which the peak current is inactivated by half, and a is the slope factor. The best fit yielded a $V_{0.5} = -57.9$ mV and an $a = 7.9$ mV/e-fold for fresh human fetal cells (●, continuous

curve), and a $V_{0.5} = -53.6$ mV and an $a = 10.5$ mV/e-fold for cultured human adult cells (■, interrupted curve). The best fit curve for cultured cells was shifted slightly positive from the curve for fresh fetal cells, but still matched reasonably well.

We studied time dependence of recovery from inactivation of the current in fresh fetal cells by increasing the interval between two identical depolarizing pulses of

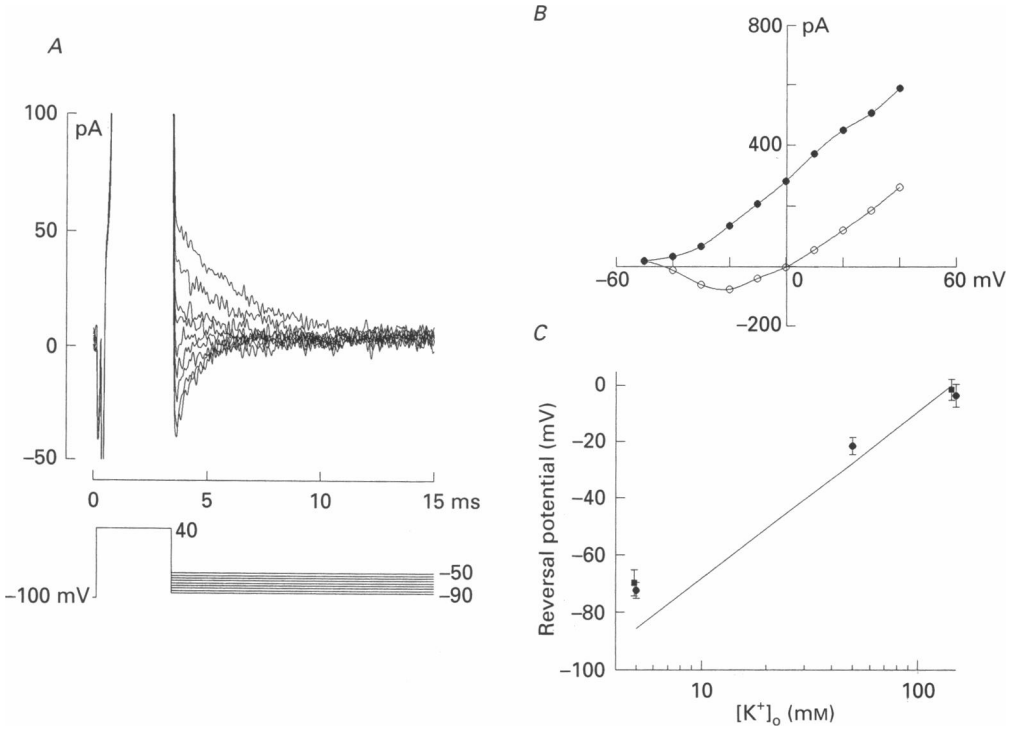

Fig. 11. Reversal potential of the transient outward current. Panel *A*, a family of tail currents recorded in 5 mM $[K^+]_o$. The membrane potential was first depolarized to +40 mV for 3 ms (V_h −100 mV) to activate the current and immediately stepped to test potentials ranging from −90 to −50 mV in 5 mV increments. Tail currents were measured 1 ms after the onset of the test steps (average of 20 data points). The interpolated zero intercept in an *I–V* plot (not shown) was taken as the reversal potential. The reversal potential of the tail current family in this figure is −75·6 mV. Some current records were omitted for clarity. Panel *B*, representative current–voltage relationships of the transient outward current in 5 mM $[K^+]_o$ (●) and in 150 mM $[K^+]_o$ (○). The current was evoked by depolarizing a cell to potentials ranging from −50 to +50 mV in 10 mV increments (V_h −100 mV) in 5 mM $[K^+]_o$. Another family of currents was recorded 5 min after the solution was changed to 150 mM $[K^+]_o$. The interpolated zero-current potential in this cell in 150 mM $[K^+]_o$ was +0·5 mV. Panel *C* is a semilogarithmic plot of reversal potentials of the transient outward current in fresh fetal cells and in cultured adult cells (●, fresh fetal cells; ■, cultured adult cells). The continuous line represents E_K.

+50 mV and observing the recovery in current amplitude of the second pulse response. Peak current to the second pulse (I_t) was normalized to peak current to the first pulse (I_{max}) and plotted in Fig. 10*C* as a function of the interval between the two pulses. The continuous curve through data points is the best fit to the equation

$$I_t/I_{max} = 1 - \exp(-t/\tau), \quad (8)$$

where t is the interval and τ is the time constant of the recovery process. The recovery process from inactivation followed a single exponential time course with a τ of 71·0 ms.

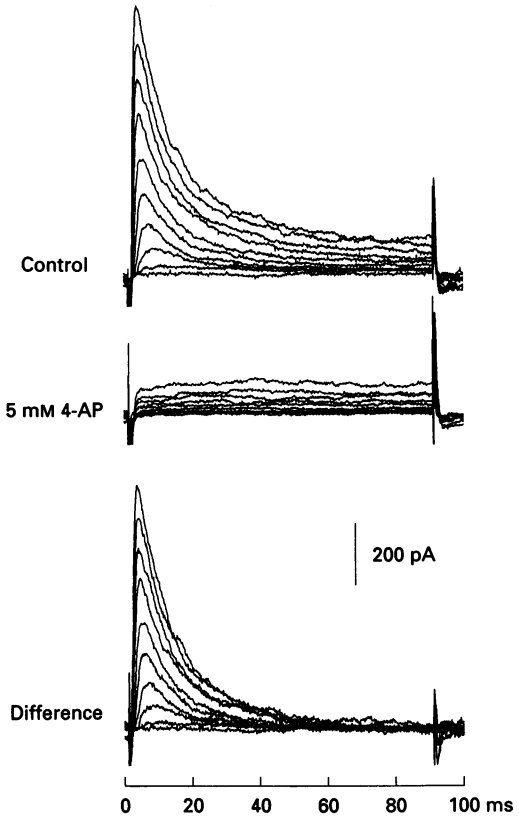

Fig. 12. Effects of 4-AP. A control current family was recorded from a fresh human fetal cell (top panel). Another current family (middle panel) was recorded 2 min after 4-AP application. The transient current was completely blocked by 4-AP at this concentration. Net 4-AP-sensitive current (lower panel) was obtained by subtracting the residual current after 4-AP treatment from control current.

Reversal potential and $[K^+]_o$

If the transient outward current is carried by potassium, its reversal potential should depend on the external potassium concentration $[K^+]_o$. We examined the reversal potentials of the current in three external potassium concentrations: 5, 50 and 150 mM (5 and 150 mM for cultured cells) using tail-current analysis (5 and 50 mM) and peak analysis (150 mM). Figure 11*A* shows a representative family of tail currents in 5 mM $[K^+]_o$. The cells were held at -100 mV and depolarized to $+40$ mV for 3 ms to activate the main current, and then stepped to test potentials from -90 to -50 mV in 5 mV increments. Tail currents were measured and the zero current potential in an I–V plot (not shown) was taken as the reversal potential. Figure 11*B* shows representative current–voltage relationships in 5 and 150 mM $[K^+]_o$. In

150 mM $[K^+]_o$ (○), when the membrane was clamped to more negative than 0 mV, the current was inward, but it became outward as the membrane potential became more positive than 0 mV. The zero current potential in an I–V plot was taken as the reversal potential. Figure 11C is a semilogarithmic plot of reversal potential against $[K^+]_o$. In 5 mM $[K^+]_o$, the reversal potential was: $-72{\cdot}4 \pm 2{\cdot}8$ mV ($n = 3$) for fresh fetal cells and $-69{\cdot}8 \pm 4{\cdot}5$ mV ($n = 4$) for cultured cells; in 50 mM $[K^+]_o$, $-21{\cdot}6 \pm 3{\cdot}0$ mV ($n = 3$) for fresh fetal cells; and in 150 mM $[K^+]_o$, $-3{\cdot}6 \pm 4{\cdot}1$ mV for fresh fetal cells, $-1{\cdot}4 \pm 3{\cdot}8$ mV ($n = 4$) for cultured cells. Since the reversal potential of the current in each $[K^+]_o$ was close to E_K, we conclude that this transient outward current was carried mostly by potassium.

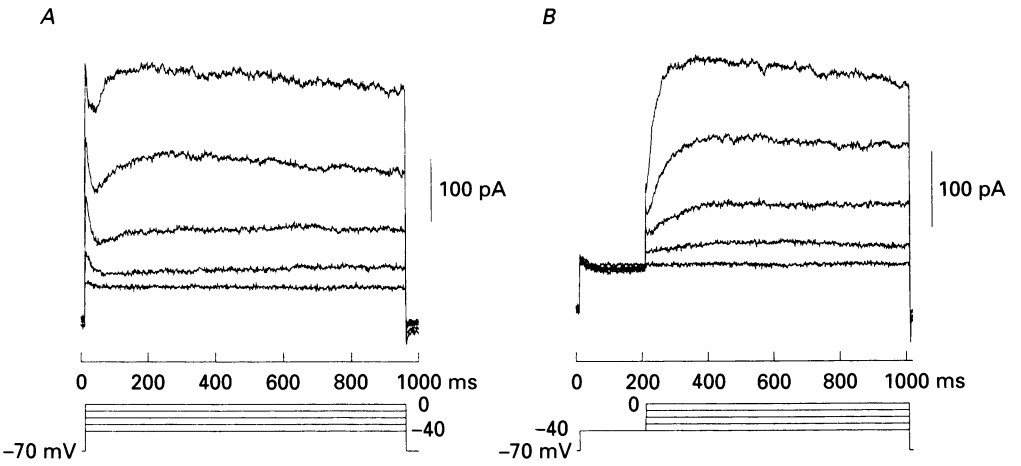

Fig. 13. The slow-activating outward current. In panel A, depolarizing pulses first evoked the transient outward current, followed by a slow-activating outward current. A prepulse of −40 mV, which inactivated 90% of the transient current (see Fig. 10B), separated the slow-activating outward current from the transient current (panel B).

Effects of external K^+ channel blockers

We investigated effects of several K^+ channel blockers (4-AP, TEA, Cs^+, and Ba^{2+}). With 1 mM 4-AP, the current was inhibited by about half (47 ± 8%, $n = 3$). Complete inhibition was achieved by 5 mM 4-AP. Figure 12 shows representative results recorded from a fresh human fetal cell. First, a family of currents (top panel) was evoked by a series of voltage pulses from −50 to +40 mV in 10 mV increments (V_h −100 mV), as control. Another current family was then recorded 2 min after application of 5 mM 4-AP (middle panel) using the same voltage-clamp protocol. With 5 mM 4-AP, the transient current was completely blocked, leaving only a small residual current. The full 4-AP-sensitive current was obtained by subtracting the residual current after 4-AP treatment from the control current (lower panel). Similar results were obtained from cultured human adult cells (not shown). In contrast, 20 mM TEA had no effect on the current. The other two K^+ channel blockers, Cs^+ and Ba^{2+} at a concentration of 2 mM, also failed to block the current when applied externally.

Non-dependence on calcium

One of the fast transient potassium currents is known to be Ca^{2+} dependent (MacDermott & Weight, 1982; Salkoff, 1983). Since in our experiments, the intracellular free Ca^{2+} concentration ($[Ca^{2+}]_i$) was kept very low (*ca* 10^{-8} M), it was unlikely that the current we observed was Ca^{2+} dependent. We further studied the calcium dependence of the current in fresh human fetal cells by removing calcium from the external solution and adding cobalt, a calcium channel blocker. We concluded that the fast transient outward potassium current in human fetal RPE cells was not calcium dependent.

Slowly activating outward current

Another outward current co-existed with the transient outward current in about 26% of the fresh fetal human cells studied (Fig. 13*A*). This current activated more slowly and resembled the delayed rectifier. A prepulse of −40 mV suppressed most of the transient outward current, leaving the slow-activating current almost intact (Fig. 13*B*). Tail current analysis showed that the reversal potential of the slow-activating current was about −70 mV in normal external solution ($[K^+]_o$ = 5 mM), suggesting that it was a potassium current.

DISCUSSION

We studied membrane potassium currents in freshly isolated human (adult and fetal) and monkey (adult) RPE cells and compared them with currents in cultured human and monkey cells of adult origin. In freshly isolated adult cells of the two species, two currents were observed in every cell we recorded: a delayed rectifier and an inward rectifier. The electrophysiological properties of each current in adult cells of the two species were virtually indistinguishable. In freshly isolated human fetal cells, however, membrane currents were remarkably different. A transient outward current, the A-current, was found to be the dominant current in all the cells, while the delayed rectifier and inward rectifier were absent in most of the fetal cells.

All three currents were found in cultured human and monkey cells. Two of them, the delayed outward rectifier and the inward rectifier, were similar to those found in fresh cells, although there were some differences in their kinetic properties. Of particular interest is that 33% of cultured human cells of adult origin expressed the A-current, which was almost identical to the A-current in fresh fetal cells.

Delayed rectifier

The delayed rectifier currents in both fresh and cultured human and monkey RPE cells activated with membrane depolarizations positive to about −30 mV (currents in cultured cells activated at more positive voltages). The current followed a sigmoidal time course to reach its steady state after a brief delay, and was virtually non-inactivating. The reversal potential of the current closely followed the potassium equilibrium potential through a wide range, indicating that the membrane channels underlying the current are highly selective for potassium. Furthermore, the currents were blocked by the potassium channel blocker, TEA. It is unlikely that these currents were Ca^{2+} dependent, since in our experiments, $[Ca^{2+}]_i$ was well buffered.

In many aspects, this current resembled the delayed rectifier type of potassium current first observed in squid neurons and widely found in other excitable cells. This current has also been identified in various non-excitable cells, including lymphocytes, glial cells, osteoblasts, hepatocytes, and even plant cells (for reviews, see Kolb, 1990; Hille, 1992). Recent whole-cell patch clamp studies in freshly isolated RPE cells in frog (Hughes & Steinberg, 1990), turtle (Fox & Steinberg, 1992), and rat (L. Botchkin, B. A. Hughes & R. H. Steinberg, unpublished observations) also identified outward K^+ currents. While the currents in human and monkey cells were virtually non-inactivating, the delayed rectifiers in frog and turtle RPE cells inactivated quite rapidly. The significance of the difference in inactivation of the currents between primate and cold-blooded vertebrates is unclear.

The conductance–voltage curves of fresh human and monkey cells matched closely, as did the curves of cultured human and monkey cells. The curve of cultured human cells, however, was shifted 16 mV positive from that of fresh human cells and a similar shift (17·7 mV) occurred for cultured monkey cells. Although we do not understand the reason for the shift, its similarity in cultured cells of the two species is unlikely to be a coincidence and indicates that delayed rectifier channels in culture undergo similar changes in both human and monkey cells.

The function of delayed rectifiers in excitable cells is believed to be to repolarize the membrane during an action potential. The wide distribution of the delayed rectifier in non-excitable cells suggests that the current may have specific cellular functions. For instance, in lymphocytes (DeCoursey, Chandy, Gupta & Cahalan, 1984; Deutsch, 1988) and recently in human melanoma cells (Nilius & Wohlrab, 1992), the delayed rectifier was found to be involved in the regulation of cell proliferation. Takumi, Ohkubo & Nakanishi, (1988) isolated a cDNA clone from rat kidney that predicted a protein of only 130 amino acids and induced an outwardly rectifying potassium current in *Xenopus* oocytes. Subsequent study showed that this potassium channel was located on the apical membrane of epithelial cells in rat kidney proximal tubule, the submandibular duct, and the uterine endometrium, suggesting that it might be involved in epithelial K^+ transport (Sugimoto *et al.* 1990). The precise function of the current in RPE cells is unknown. Certainly, if the membrane potential were depolarized to a level sufficient to activate the delayed rectifier, this current would help repolarize the membrane back to the resting level.

Inward rectifier

The inward rectifier was observed in fresh adult and cultured cells of both species. The activation of the current was virtually time independent. The zero-current potential of the current was close to E_K in $[K^+]_o$ from 1 to 25 mM, indicating that potassium is the major carrier. The inhibitory effects of the potassium channel blockers Ba^{2+} and Cs^+ on this current also support that it is a potassium current. Similar inward rectifiers have been recorded in fresh frog RPE cells (Hughes & Steinberg, 1990).

One major difference between the currents in fresh and in cultured cells is that the current in cultured cells inactivated when hyperpolarizing pulses were more negative than -120 mV. Such inactivation was never observed in fresh cells. The inactivation is believed to be due to the blocking effect of external Na^+ at very negative

hyperpolarizations (Ohmori, 1978; Biermans *et al.* 1988), and in our experiments, this inactivation was removed in a Na^+-free solution. Similar inactivation was observed in other cells. We do not know the cause of the difference between fresh and cultured RPE cells regarding inactivation of the inward rectifier. That inactivation was found in cultured RPE cells of both species but not in fresh cells indicates, again, that both human and monkey RPE cells undergo similar changes in culture.

Inward rectifiers have been found in a wide variety of excitable and non-excitable cells. The function of this current is believed to be to maintain a resting potential near E_K (for reviews, see Kolb, 1990; Hille, 1992), and to counter local elevations in extracellular potassium (Barres, Chun & Corey, 1990; Barres, 1991; Chiu, 1991). The inward rectifier in RPE cells yields outward current when the membrane potential is more positive than E_K, so that when the membrane potential moves slightly away from E_K this current can help bring the membrane potential back to E_K. Indeed, the resting potential has been found near E_K in frog RPE cells (Miller & Steinberg, 1977*b*), where an inward rectifier has been identified (Hughes & Steinberg, 1990). In some freshly isolated human and monkey RPE cells, the resting potentials were around -65 mV, reasonably close to E_K. This current could also play a role in the homeostasis of potassium levels in the subretinal space, especially during light-evoked subretinal potassium fluctuations (Oakley & Green, 1976).

A-current

This current was found to be the dominant membrane current in fresh human fetal cells and was observed in every recorded cell. It was also found in 33% of the cultured human cells of adult origin, but only in one cultured adult monkey cell out of over eighty cells we recorded from. Its kinetic and pharmacological properties resembled the A-type potassium current found in excitable cells, and its reversal potential followed E_K closely for a wide range of $[K^+]_o$, indicating that it was a potassium current. This current was blocked by 4-AP, but not by TEA, Cs^+, or Ba^{2+}, and it was not Ca^{2+} dependent.

The A-current was first observed in molluscan neurons and has since been found in most excitable cells, including mammalian central neurons (for reviews, see Rogawski, 1985; Rudy, 1988). This current has also been described in non-excitable cells, including glial cells (for a review, see Barres *et al.* 1990). Many genes have been cloned that encode for A-type potassium channels (for reviews, see Jan & Jan, 1989, 1990). In excitable cells, the functional roles of the A-current are believed to include frequency regulation of firing (frequency encoding), spike repolarization, and modulation of synaptic transmission (Rogawski, 1985), but its functions in non-excitable cells are not yet clear.

Developmental regulation of membrane channel phenotype in human RPE cells

Although we found that the A-current was prominent in fresh human fetal cells, we never recorded this current in any fresh adult cells. The remarkable difference in membrane channel patterns between fresh fetal and adult human RPE cells clearly points out that membrane channel phenotype changes during RPE maturation, and

the co-existence of the A-current and delayed rectifier in 26% of the fetal cells may indicate an intermediate stage between fetal and adult RPE.

Changes in membrane channel phenotype during development have been observed in various cell types. For instance, in the dorsal longitudinal flight muscles of *Drosophila*, the A-current develops first, followed by the delayed rectifier (Salkoff & Wyman, 1983). Butler, Wei, Baker & Salkoff (1989) found that in *Drosophila*, a gene encoding for potassium channels, *Shab*, was expressed in late embryonic and pupa stages, but not in adult animals. In vertebrate skeletal muscles, innervation is followed by a major change in membrane channel phenotype to the adult type. Interestingly, this change can be reversed under certain conditions: a dramatic increase in embryonic types of membrane channels can be seen within a week of denervation (see Hille, 1992).

Perhaps one of the best examples of a change in membrane-channel phenotype comes from studies of murine T cell development (Lewis & Cahalan, 1988). Most functionally immature thymocytes (CD4-CD8$^-$ or CD4$^+$CD8$^+$ cells) express large numbers of type *n* channels, a delayed rectifier-like channel. When the cells reach maturity, changes in channel phenotype occur that depend upon the functional class of cell. CD4$^+$CD8$^-$ cells (most of them helper T cells) express type *n* channels, but ten times fewer in number than immature cells, while CD4$^-$CD8$^+$ cells (primarily cytotoxic and suppressor T cells) display types *n'* and *l* channels that differ from type *n* channels. When activated, both CD4$^+$CD8$^-$ and CD4$^-$CD8$^+$ cells express type *n* channels again at a level comparable to immature cells, regardless of which channels they expressed previously.

The functional significance of changes in membrane-channel phenotype during development of RPE cells is not clear. Since both RPE and neural retina share the same origin in neuroepithelium of the optic vesicle, an outgrowth of the forebrain neuroepithelium, we can speculate that primitive neuroepithelial cells in the early developing eye exhibit neuronal characteristics and that, perhaps, the A-current is one of them. The disappearance of the A-current in adult cells could indicate cell maturation toward the RPE phenotype.

The occurrence of the A-current in cultured RPE cells

Since the A-current disappears when RPE cells mature, the expression of A-current in cultured cells of adult origin may indicate a reversal of this maturation process. These findings are consistent with those of Neill & Barnstable (1990) for rat RPE cells in culture, which led to their suggesting a dedifferentiation model. They found that embryonic rat RPE cells expressed the cell adhesion molecule N-CAM but ceased to express it as they matured. When N-CAM-negative rat RPE cells were grown in culture, they re-expressed the molecule. In our experiments, some cultured RPE cells also expressed a TTX-sensitive sodium current, which was absent in fresh adult cells (R. Wen & R. H. Steinberg, unpublished observations). Since this current has not been observed in fresh fetal RPE cells (16–21 weeks), its significance with respect to the dedifferentiation idea is not clear. Our finding that cultured adult human RPE cells appear to re-express a more primitive neuroepithelial membrane channel phenotype may be one step toward the regenerative capability observed in other species.

We thank Drs Julie L. Schnapf, Timothy W. Kraft and David M. Schneeweis for helping us to obtain adult human and monkey tissues; Drs Henry J. Ralston III and Diane B. Ralston for providing us with monkey tissue; and Drs Robert B. Jaffe, Sam Mesiamo, and Ms Cindy Voytek for providing us with human fetal tissue. Dr Karl-Heinz Huemer participated in some of the work. This work was supported by NIH grant EY01429.

REFERENCES

BARRES, B. A. (1991). New roles for glia. *Journal of Neuroscience* **11**, 3685–3694.

BARRES, B. A., CHUN, L. L. Y. & COREY, D. P. (1990). Ion channels in vertebrate glia. *Annual Review of Neuroscience* **13**, 441–474.

BIERMANS, G., VEREECKE, J. & CARMELIET, E. (1988). The mechanism of inactivation of the inward-rectifying K current during hyperpolarizing steps in guinea-pig ventricular myocytes. *Pflügers Archiv* **410**, 604–613.

BUTLER, A., WEI, A., BAKER, K. & SALKOFF, L. (1989). A family of putative potassium channel genes in *Drosophila*. *Science* **243**, 943–947.

CHIU, S. Y. (1991). Functions and distribution of voltage-gated sodium and potassium channels in mammalian Schwann cells. *Glia* **4**, 541–558.

COREY, D. P. & STEVENS, C. F. (1983). Science and technology of patch-recording electrodes. In *Single-Channel Recording*, ed. SAKMANN, B. & NEHER, E., pp. 53–68. Plenum Press, New York.

DECOURSEY, T. E., CHANDY, K. G., GUPTA, S. & CAHALAN, M. D. (1984). Voltage-gated K^+ channels in human T lymphocytes: a role in mitogenesis? *Nature* **307**, 465–468.

DEUTSCH, C. (1988). K^+ channels and mitogenesis. In *Potassium Channels: Basic Function and Therapeutic Aspects*, ed. COLATSK, T. J., pp. 251–271. Wiley-Liss, New York.

FOX, J. A., PFEFFER, B. A. & FAIN, G. L. (1988). Single-channel recordings from cultured human retinal pigment epithelial cells. *Journal of General Physiology* **91**, 193–222.

FOX, J. A. & STEINBERG, R. H. (1992). Voltage-dependent currents in isolated cells of the turtle retinal pigment epithelium. *Pflügers Archiv* **402**, 451–60.

HAMILL, O. P., MARTY, A., NEHER, E., SAKMANN, B. & SIGWORTH, F. J. (1981). Improved patch-clamp techniques for high-resolution current recording from cells and cell-free membrane patches. *Pflügers Archiv* **391**, 85–100.

HILLE, B. (1992). *Ionic Channels of Excitable Membranes*. Sinauer Associates Inc., Sunderland, MA, USA.

HODGKIN, A. K. & HUXLEY, A. F. (1952). A quantitative description of membrane current and its application to conduction and excitation in nerve. *Journal of Physiology* **117**, 500–544.

HUGHES, B. A. & STEINBERG, R. H. (1990). Voltage-dependent currents in isolated cells of the frog retinal pigment epithelium. *Journal of Physiology* **428**, 273–297.

JAN, L. Y. & JAN, Y. N. (1989). Voltage-sensitive ion channels. *Cell* **56**, 13–25.

JAN, L. Y. & JAN, Y. N. (1990). How might the diversity of potassium channels be generated? *Trends in Neurosciences* **13**, 415–419.

JAUCH, P., PETERSON, O. H. & LÄUGER, P. (1986). Electrogenic properties of the sodium–alanine cotransporter in pancreatic acinar cells: I. Tight-seal whole-cell recordings. *Journal of Membrane Biology* **94**, 99–115.

KOLB, H. (1990). Potassium channels in excitable and non-excitable cells. *Reviews of Physiology, Biochemistry and Pharmacology* **115**, 52–91.

LA COUR, M., LUND-ANDERSEN, H. & ZEUTHEN, T. (1986). Potassium transport of the frog retinal pigment epithelium: autoregulation of potassium activity in the subretinal space. *Journal of Physiology* **375**, 461–479.

LEWIS, R. S. & CAHALAN, M. D. (1988). The plasticity of ion channels: parallels between the nervous and immune systems. *Trends in Neurosciences* **11**, 214–218.

LIN, H., KENYON, E. & MILLER, S. S. (1992). Na-dependent pH_i regulatory mechanisms in native human retinal pigment epithelium. *Investigative Ophthalmology and Visual Science* **33**, 3528–3538.

MACDERMOTT, A. B. & WEIGHT, F. F. (1982). Action potential repolarization may involve a transient Ca^{2+}-sensitive outward current in a vertebrate neuron. *Nature* **300**, 185–188.

MILLER, S. S. & STEINBERG, R. H. (1977*a*). Active transport of ions across frog retinal pigment epithelium. *Experimental Eye Research* **25**, 235–248.

MILLER, S. S. & STEINBERG, R. H. (1977*b*). Passive ionic properties of frog retinal pigment epithelium. *Journal of Membrane Biology* **36**, 337–372.

NEILL, J. M. & BARNSTABLE, C. J. (1990). Expression of the cell surface antigens RET-PE2 and N-CAM by rat retinal pigment epithelial cells during development and in tissue culture. *Experimental Eye Research* **51**, 573–583.

NILIUS, B. & WOHLRAB, W. (1992). Potassium channels and regulation of proliferation of human melanoma cells. *Journal of Physiology* **445**, 537–548.

OAKLEY, B. II. & GREEN, D. G. (1976). Correlation of light-induced changes in retinal extracellular potassium concentration with the c-wave of the electroretinogram. *Journal of Neurophysiology* **39**, 1117–1133.

OAKLEY, B. II., MILLER, S. S. & STEINBERG, R. H. (1978). Effect of intracellular potassium upon the electrogenic pump of the frog retinal pigment epithelium. *Journal of Membrane Biology* **44**, 281–302.

OHMORI, H. (1978). Inactivation kinetics and steady-state current noise in the anomalous rectifier of tunicate egg cell membranes. *Journal of Physiology* **218**, 77–99.

QUINN, R. H. & MILLER, S. S. (1992). Ion transport mechanisms in native human retinal pigment epithelium. *Investigative Ophthalmology and Visual Science* **33**, 3513–3527.

ROGAWSKI, M. A. (1985). The A-current: how ubiquitous a feature of excitable cells is it? *Trends in Neurosciences* **8**, 214–219.

RUDY, B. (1988). Diversity and ubiquity of K channels. *Neuroscience* **25**, 729–749.

SALKOFF, L. (1983). *Drosophila* mutants reveal two components of fast outward current. *Nature* **302**, 249–251.

SALKOFF, L. & WYMAN, R. (1983). Ion currents in *Drosophila* flight muscles. *Journal of Physiology* **337**, 687–709.

SONG, M. & LUI, G. M. (1990). Propagation of fetal human RPE cells: preservation of original culture morphology after serial passage. *Journal of Cellular Physiology* **143**, 196–203.

STEINBERG, R. H. (1988). Electrical interactions between the RPE and the photoreceptors. In *Retinal Diseases – Biomedical Foundations and Clinical Management*, ed. TSO, M. M., pp. 60–79. J. B. Lippincott Co., Philadelphia.

SUGIMOTO, T., TANABE, Y., SHIGEMOTO, R., IWAI, M., TAKUMI, T., OHKUBO, H. & NAKANISHI, S. (1990). Immunohistochemical study of a rat membrane protein which induces a selective potassium permeation: its localization in the apical membrane portion of epithelial cells. *Journal of Membrane Biology* **113**, 39–47.

TAKUMI, T., OHKUBO, H. & NAKANISHI, S. (1988). Cloning of a membrane protein that induces a slow voltage-gated potassium current. *Science* **242**, 1042–1045.

WEN, R., LUI, G. M. & STEINBERG, R. H. (1991*a*). Voltage-dependent current in cultured human retinal pigment epithelial cells. *Biophysical Journal* **59**, 648a.

WEN, R., LUI, G. M. & STEINBERG, R. H. (1991*b*). Voltage-dependent whole cell currents in cultured human and monkey RPE cells. *Investigative Ophthalmology and Visual Science* **32**, 617.